A Sensor-Based Sun-Tracking Energy Harvest System

Chia-Hung Tsai

Department of Computer Science,
National Chiao Tung University, Hsin-Chu, 30010, Taiwan
Email:chiahung@cs.nctu.edu.tw

Shu-Chiung Hu

Department of Computer Science,
National Chiao Tung University, Hsin-Chu, 30010, Taiwan
Email:schu@cs.nctu.edu.tw

Chung-Hsiang Huang

Department of Computer Science,
National Chiao Tung University, Hsin-Chu, 30010, Taiwan
Email:chhhuang@cs.nctu.edu.tw

Yu-Chee Tseng*

Department of Computer Science,
National Chiao Tung University, Hsin-Chu, 30010, Taiwan
Email:yctseng@cs.nctu.edu.tw
*Corresponding author

Abstract: Recent study has shown that the energy gain of a solar panel will be significantly influenced by the incidence angle of the sun radiation. The main goal of this paper is to present a sensor-based sun-tracking system. First, we design a sensing tower for measuring the direction of sun radiation. Then we design a sun-tracking algorithm, which adopts an iterative process to identify the direction of sun radiation to the earth's surface. This information is then passed to the nearby solar panels to adjust their angles. We have also developed a prototype and conducted several simulations to verify our sun-tracking system. Simulation results show that our system has better performance on the solar energy generation than existing ones.

Keywords: Energy harvest, green energy, renewable energy, sensing technology, sun tracking.

Reference to this paper should be made as follows: Tsai, C.-H., Hu, S.-C., Huang, C.-H., and Tseng, Y.-C. (xxxx) 'A Sensor-Based Sun-Tracking Energy Harvest System', *Int. J. Sensor Networks*, Vol. x, No. x, pp.xxx–xxx.

Biographical notes:

Chia-Hung Tsai received his M.S. and Ph.D. degrees in Computer Science and Information Engineering from the National Chiao Tung University, Taiwan, in 2006 and 2012, respectively. His research interests include wireless communication and sensor networks.

Shu-Chiung Hu received her B.S. degree in Computer Science from Tung-Hai University, Taiwan, in 2003. She received her M.S. degree in Computer Science and Information Engineering from National Taiwan Normal University, Taiwan, in 2006 and is currently a Ph.D. Candidate in the Department of Computer Science at the Chiao Tung University. Her research interests include wireless communication and sensor networks.

Chung-Hsiang Huang received his B.S. and M.S. degrees in computer science from the National Chiao Tung University, Taiwan, in 2008 and 2010, respectively. His research interest focuses on wireless sensor networks.

Yu-Chee Tseng received his Ph.D. in Computer and Information Science from the Ohio State University in 1994. He is Professor and Dean at the Department of Computer Science, National Chiao Tung University, Taiwan. Dr. Tseng received the Outstanding Research Award, by National Science Council, ROC, in both 2001-2002 and 2003-2005, Best Paper Award, by Intl Conf. on Parallel Processing, in 2003, the Elite I. T. Award in 2004, and Distinguished Alumnus Award, by the Ohio State University, in 2005. His research interests include mobile computing, wireless communication, and parallel and distributed computing. Dr. Tseng is a member of ACM and a Senior Member of IEEE.

1 Introduction

Conventional fossil energy sources such as petroleum, natural gas, and coal are depleting rapidly. Fossil fuels are non-renewable and the use of such resources causes greenhouse effects and pollution. Therefore, finding renewable energies has become very important. Renewable energies may come from sunlight, wind, water, tides, and geothermal heat. Among them, solar energy is one of the most important renewable and cleanest sources. Solar energy even supplies power for some sensor applications Alippi et al. (2011); Tang and Bermak (2012). However, if we want to exploit solar energy as a practical alternative to fossil fuels, we must have efficient ways to convert solar energy into electricity.

A major way to convert solar energy into electricity is to use *photovoltaic (PV) panels*, or known as *solar panels*, which have become more popular as their prices dropped recently. Nowadays, most PV panels have an energy conversion ratio of 12-18% Oner et al. (2009); SunPower (http://us.sunpowercorp.com/). For best conversion performance, most PV systems target on lengthening the time that they face the sun. As a result, solar trackers are designed to follow the sun by moving or rotating PV panels. The increase in energy conversion can be as much as 20% and 50% in winter and in summer Photovoltaics (http://en.wikipedia.org/wiki/Photovoltaics), respectively. References Abdallah and Nijmeh (2004); Lorenzo et al. (2002); Mamlook et al. (2006) have shown that an ideal sun tracker can produce about 40% more energy than an optimally tilted static panel. The efficiency also depends on the panel temperature and the incidence angle of solar radiation Clifford and Eastwood (2004); Dincer and Meral (2010). This motivates us to study panels with sun-tracking capability.

Regarding moving control capability, sun-tracking systems can be classified into two types Mousazadeh et al. (2009); Oner et al. (2009): *passive* and *active*. The passive ones do not require any electronic controls or motors but rely on fluid movement, bimetallic strips, viscous damper controlled, etc. Campos et al. (2011); Clifford and Eastwood (2004); Mwithiga and Kigo (2005)). Hence, it can only provide moderate accuracy. The active ones, however, rely on sensors and electronic controls. On the other hand, regarding the control model, sun-tracking systems can also be classified as *open-loop* or *closed-loop* Lee et al. (2009). An open-loop (algorithm-based) type of system runs based on the current state to determine if it has achieved the desired goal without using feedback. A closed-loop (sensor-based) system runs based on the feedbacks of sensors, which detect relevant parameters induced by the sun, so as to yield more accurate outputs. Such systems can track the position of the sun with the feedback of sensors, instead of using local date/time for the prediction. It even works regardless of weather conditions (such as cloud and fog). Such sensors are usually quite lightweight and cause low overhead Aiuchi et al. (2006); Jiao et al. (2010); Kalogirou (1996); Kelly and Gibson (2009).

In this work, we propose a sensing tower architecture. It executes a sun-tracking algorithm to determine the precise direction of sun radiation. Then a coordinator will evaluate whether it should command its nearby solar panels to perform sun tracking or not. The main contribution of this work is three-fold. First, our system works regardless of sunny or cloudy days. Second, our system allows a small, lightweight sensing tower to control multiple solar panels, thus incurring low costs. Third, no location and time information is needed.

The rest of this paper is organized as follows. Related work and motivations are given in Section 2. Section 3 shows our design. Section 4 verifies our system via simulation results. Section 5 demonstrates our prototype. Finally, Section 6 concludes this paper.

2 Related Work and Motivations

Sun-tracking capability can improve efficiency of solar energy harvesting. Such systems can be categorized into two types. The open-loop systems use the current state (such as the local date and time) to determine the sun's position Blanco-Muriel et al. (2006); Canada et al. (2007); Nuwayhid et al. (2001); Palavras and Bakos (2004). An astronomical almanac algorithm is proposed in Michalsky (1988). A PSA algorithm is proposed in Blanco-Muriel et al. (2006) to improve the accuracy and computing efficiency with the introduction of new coefficients and parallax correction. It reduces the standard deviation errors in zenith, azimuth, and direction of the sun by 18%, 11%, and 25%, respectively. Recently, Grena (2008) presents an algorithm taking the fractional Universal Time (UT), the date, and the difference between UT and Terrestrial Time (TT), longitude, latitude, pressure, and temperature as inputs. It can compute very precise position of the sun by taking into account the atmospherical refraction. References Chen et al. (2006) and Chong et al. (2009) propose general formulas for arbitrarily oriented sun-tracking axes for off-axis and on-axis solar collectors, respectively. Open-loop systems are simpler and cheaper than closed-loop ones but have no error correction capability.

The closed-loop systems adopt inputs from sensors. The design of such systems is more complicated. Conversion efficiency of such systems is typically better since sensors provide feedback to improve the sun-tracking precision. Moreover, some sun re-tracking mechanisms Aiuchi et al. (2006); Fontani et al. (2011); Jiao et al. (2010); Kalogirou (1996); Kelly and Gibson (2009) can be designed based on sensor feedbacks and thus they can work even in bad weather conditions (such as cloud and fog). In many closed-loop systems, image sensors and light sensors are used. References Fontani et al. (2011); Han et al. (2011); Yang et al. (2009) use image sensors (camera) to track the sun by the pinhole imaging principal. In Yang et al. (2009), an active pixel

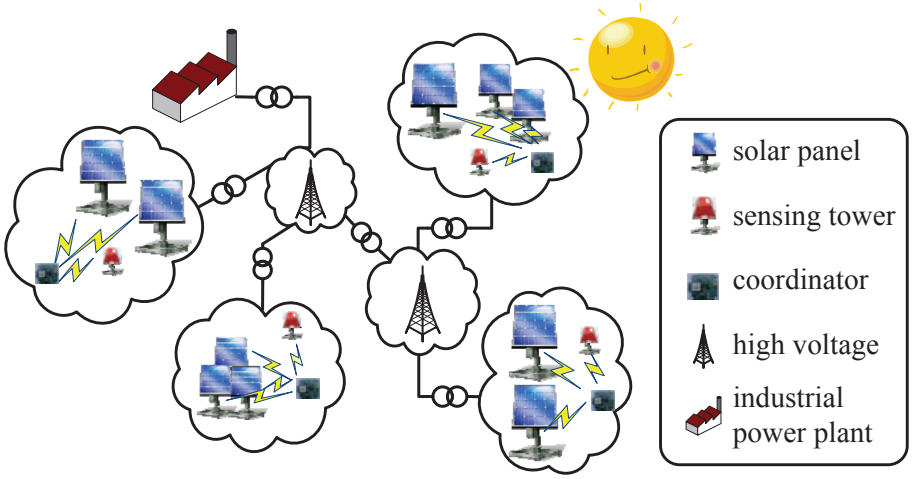

Figure 1: System architecture.

sensor (APS) is used first to coarsely point toward the sun; then a CMOS camera is used as the fine sun tracker and also the back-sunlight target detector. The work Han et al. (2011) lets the divergent sun rays pass the pinhole imaging to estimate the sun spot. A double guiding system is proposed in Fontani et al. (2011). A passive tracking device first finds the preliminary orientation, and then an active sun finder system exploits a camera without lenses composed of a pinhole sensor mounted over the detector. The active sun finder then calculates the sensor FOV aperture through the distance from the pinhole to the detector to point to the sun. The system can reassign the position when the sky transits from cloudy to clear. Reference Berenguel et al. (2004) uses CCD images to eliminate heliostats offsets and calculate the sunbeam centroid. An electro-optical sensor-based system for controlling the heliostats is proposed in Aiuchi et al. (2006), where two photo sensors are placed side by side on the bottom of a small box to rotate the heliostat. It is shown that on clear days the angular error is about 0.002 rad.

To reduce the computation and hardware costs of Aiuchi et al. (2006); Berenguel et al. (2004), several lightweight systems have been proposed. Such systems mainly drive motors when light sensors sense unbalanced illuminations. Single axis sun tracking systems are introduced in Deb and Roy (2012); Huang and Sun (2007); Ponniran et al. (2011) and bi-axial systems are introduced in Bakos (2006); Dasgupta et al. (2010); Jiao et al. (2010); Shibata and Tambo (2010). The former follows the sun's east-west movement, while the latter further follows the sun's altitude angle. A comparison of bi-axial, single-vertical-axial, single-E-W-axial, and single-N-S-axial systems is conducted in Abdallah (2004), which concludes that electrical power gains of 43.87%, 37.53%, 34.43% and 15.69% by these systems, respectively, as compared to the fixed-angle system. A dish-like solar concentration system is developed in Palavras and Bakos (2006). It shows that the temperatures in the focal region can reach 300°C and the average heat loss coefficient can reach approximately 163 W/m^2K. Although bi-axial systems outperform uni-axial systems in conversion efficiency, they sometimes may need a lot of re-tracking work. Also, as Sungur (2009) mention, such systems may enter unstable states under cloudy conditions.

Clouds, fogs, and gas may cause refraction and diffraction of solar radiation. Reference Aracil et al. (2006) points out the effect of clouds on sun-tracking systems. Under cloudy conditions, the system controller may erroneously interpret that the sun is moving to the east. References Aiuchi et al. (2006); Choi et al. (2010); Kalogirou (1996); Kelly and Gibson (2009) enforce PV panels to move at a steady, constant speed when bad weather conditions are detected. The system proposed in Fontani et al. (2011) can re-track the position of the sun when the sky transits from cloudy to clear. Contrarily, reference Jiao et al. (2010) suggests to keep the PV panel still under low illumination in a cloudy day or in sunset. However, the definition of "bad weather" is based on a fixed threshold value of the perceived illumination. How to choose the threshold is also critical to energy generation, as pointed out in Choi et al. (2010).

The above discussion has motivated us to design a sensor-based sun-tracking system that can adapt to weather conditions, evaluate the motor rotation cost as opposed to solar energy gain, and take advantage of the wireless communication technology to facilitate control jobs.

3 Design of Sensor-Based Sun-Tracking System

3.1 System Architecture

Fig. 1 shows our sun-tracking system architecture. It consists of some solar panels, coordinators, and sensing towers. Each solar panel is rotatable in that it has a motor to change its direction. Each coordinator

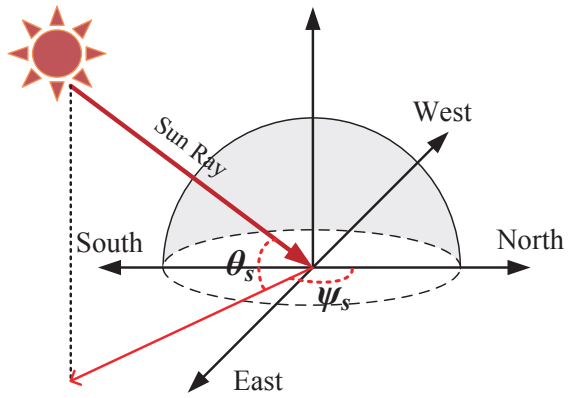

Figure 2: The solar azimuth angle ψ_s and the solar altitude angle θ_s.

controls a set of solar panels and a sensing tower. Each sensing tower has multiple photo-sensor boards assembled together to calculate the current sun radiation direction and illumination level. Each sensing tower is also self-rotatable. It can adjust its direction from time to time, by our proposed iterative sun-tracking algorithm, to determine the actual arrival angle of sun radiation. Each tower will perform the sun-tracking procedure periodically and report the direction of sun radiation and the illumination level that it sensed to its coordinator. The coordinator then instructs nearby panels, if worthy, to adjust their directions to harvest solar energies. Note that sensing towers are quite small and thus the corresponding rotation cost is negligible.

There are three parts in our system: 1) sensing tower, 2) sun-tracking algorithm, and 3) rotation decision. They are discussed in the following sections.

3.2 Sensing Tower

The earth has two movements: rotation around the sun and rotation around its own axis. This causes different solar positions at different locations and time. The position of the sun can be represented by two different angles: *azimuth angle* and *altitude angle*. Fig. 2 shows an example. The former is the angle, along the clockwise direction, from due north to the line extending from the observer to the projected location of the sun on the ground. Its largest value is 228° (occurred on June 21st in the Northern hemisphere) and its smallest value is 37.6° (occurred on December 22nd) Sungur (2009). The latter is the angle from the line extending from the observer to the projected location of the sun on the ground, to the line extending from the observer to the sun. Its range is 0° to 90°. A naive design of the sensing tower is to build a hemisphere on which dense photo-sensors are deployed, as shown in Fig. 3(a). Then the sensor which receives the maximum illumination value would reflect the direction of sun radiation. To reduce the number of sensors required, we pick only k sensors from the above naive solution that are evenly distributed on the hemisphere. We show our design of $k = 5$ in Fig. 3(b), where sensor S_1 is placed on the top of the hemisphere ($\psi_1 = 0$ and $\theta_1 = \frac{\pi}{2}$) and sensors S_2, S_3, S_4, and S_5 are four sensors with azimuth angles $\psi_2 = 0$, $\psi_3 = \frac{\pi}{2}$, $\psi_4 = \pi$, and $\psi_5 = \frac{3\pi}{2}$, respectively, and altitude angles $\theta_2 = \theta_3 = \theta_4 = \theta_5 = \frac{\pi}{3}$. Fig. 3(c) shows how to put these sensors on a pyramid-like tower with five planes, each tangent to the hemisphere. We can easily extend the design to other values of k.

Here we adopt the solar coordinate system to denote our sensors. The azimuth reference plane is defined as north-east plane (instead of the general x-y plane). The zenith reference is defined as the z-axis. Hence, the coordinate of each sensor can be defined by its azimuth angle, altitude angle, and the radius of the hemisphere. For example, in Fig. 3(c), the coordinate of sensor S_1 is (r, θ_1, ψ_1), where r is the radius. Note that since we are only interested in the arrival angle of sun radiation, the value of r is not essential. The only restriction is that one sensor is on the top and the other sensors are distributed evenly and symmetrically on the hemisphere.

3.3 Sun-Tracking Algorithm

Because sun radiation may cause the reflection and refraction, the main goal of our sun-tracking system is to identify the direction receiving the maximal energy. The core concept is based on the center of mass. Assume that S_1 is on the top and $S_2, S_3, \ldots, S_k$ are evenly distributed on the hemisphere. Our algorithm will try to point S_1 toward the direction of sun radiation. Our algorithm can start from any initial direction of the hemisphere. Let us denote by (r, θ_i, ψ_i) the current location of sensor S_i. Our algorithm has an iterative process and after each iteration, let (r_M, θ_M, ψ_M) be the center of mass of all sensors. The iteration stops when $|\theta_1 - \theta_M| \leq \theta_\epsilon$ and $|\psi_1 - \psi_M| \leq \psi_\epsilon$, where θ_ϵ and ψ_ϵ are two small threshold values. The detail of one iteration is presented below.

1. First, we translate each sensor's coordinate to the *Cartesian coordinate system*. For each sensor S_i $(i = 1, 2, \ldots, k)$, its Cartesian coordinate (x_i, y_i, z_i) can be written as

$$\begin{aligned} x_i &= r\cos(\theta_i)\cos(\psi_i), \\ y_i &= r\cos(\theta_i)\sin(\psi_i), \\ z_i &= r\sin(\theta_i). \end{aligned} \tag{1}$$

2. We adopt a weighted method to calculate the center of mass M of these k sensors:

$$(x_M, y_M, z_M) = \frac{\sum_{i=1}^{k} L_i \times (x_i, y_i, z_i)}{\sum_{i=1}^{k} L_i}, \tag{2}$$

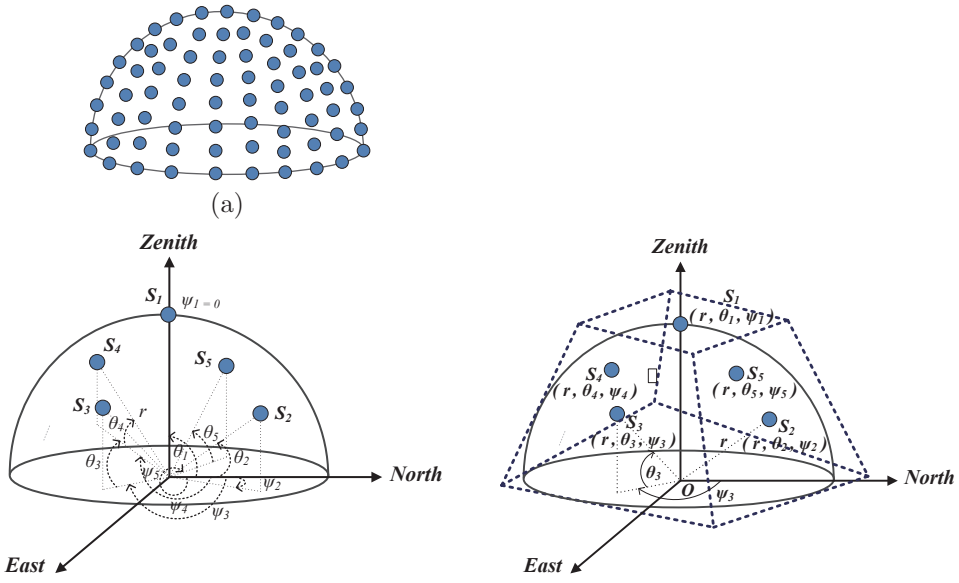

Figure 3: Design of sensing towers: (a) a naive solution with dense sensors, (b) $k = 5$ sensors and their azimuth and altitude angles, and (c) a pyramid-like sensing tower with $k = 5$.

where L_i is the current illumination level perceived by S_i. We then convert the coordinator of M to the spherical coordinate (r_M, θ_M, ψ_M) as follows:

$$\begin{aligned} r_M &= \sqrt{x_M^2 + y_M^2 + z_M^2}, \\ \theta_M &= \arccos \frac{z_M}{r'}, \\ \psi_M &= \begin{cases} \arccos \frac{x_M}{\sin \theta_M}, & \text{if } y_M \geq 0 \\ 2\pi - \arccos \frac{x_M}{\sin \theta_M}, & \text{otherwise.} \end{cases} \end{aligned} \tag{3}$$

3. Then we can calculate the rotation altitude angle $\Delta\theta$ and azimuth angle $\Delta\psi$ as follows.

$$\begin{aligned} \Delta\theta &= \theta_M - \theta_1, \\ \Delta\psi &= \psi_M - \psi_1. \end{aligned} \tag{4}$$

4. After the rotation in step 3, if both $\Delta\theta \leq \theta_\epsilon$ and $\Delta\psi \leq \psi_\epsilon$, the process is terminated and the sensing tower will report its new θ_1 and ψ_1 and the new illumination level L_1' back to the coordinator. Otherwise, the sensing tower rotates itself by $\Delta\theta$ and $\Delta\psi$. After that, each sensor also rotates to a new location on the hemisphere. Then go back to step 1 and repeat the iterative process again.

3.4 Rotation Decision of Solar Panels

Next, we discuss how the coordinator improves the energy gain of its solar panels even under cloudy conditions. We assume that two stepper motors are adopted by each solar panel with one for azimuth movement and the other for altitude movement. We also assume that P_{az} Watt and P_{al} Watt are needed to rotate a panel by d_{az} degrees and d_{al} degrees, respectively. The rotation decision is to compare the energies to be harvested between making the rotation and remaining unchanged. Assume that our system performs the sun-tracking procedure every T interval. After the coordinator receives θ_1, ψ_1, and L_1' from its sensing tower, the energy gain $E_{rotation}$ by making the rotation decision can be estimated as follows:

$$E_{rotation} = E(L_1') \times T,$$

where $E(x)$ is the power generation rate of the solar panel by perceiving x illumination per second. On the other hand, let L_p be the illumination value perceived by the solar panel. The energy gain $E_{unchanged}$ by remaining unchanged can be determined below:

$$E_{unchanged} = E(L_p) \times T.$$

Finally, the energy consumption by rotating the solar panel should be taken into consideration. Based on our solar coordinate system, we denote the altitude angle θ_p and azimuth angle ψ_p of the solar panel as the altitude and azimuth angles of its normal vector, respectively. The rotation cost E_{cost} by making the rotation decision can be calculated by Eq. (5).

$$E_{cost} = P_{az} \times \frac{|\psi_p - \psi_1|}{d_{az} \times \frac{2\pi}{360^\circ}} + \quad P_{al} \times \frac{|\theta_p - \theta_1|}{d_{al} \times \frac{2\pi}{360^\circ}}. \tag{5}$$

Then if $(E_{rotation} - E_{cost}) > E_{unchanged}$, the coordinator will decide to instruct its panels to adjust their directions. Otherwise, no change is made.

4 Simulation Results

A simulator has been implemented based on C language. For simulating the solar azimuth and altitude angles of sun radiation, we use *SOLPOS* as our solar radiation model, which is developed by National Renewable Energy Laboratory (NREL). GOLPOS can calculate the solar position and the intensity (theoretical maximum solar energy) by given date, time, and location information on earth. In the simulation, the location is set on (CCT-08:00120E58'00"24N48'00") in Hsin-Chu city, Taiwan. For verifying the performance of our sun-tracking approach, we compare the precision of the estimated direction of sun radiation, the energy consumption, and the energy generation during the tracking period with four sun-tracking approaches: 1) our approach (*Ours*), 2) *Gradient Method (GM)* proposed in Peterson et al. (2005), 3) one with a fixed solar panel (*Fixed*), and 4) one with fixed altitude angles and constant rotation speed (*Const*). Besides, we further measure the tracking time required by our sensing tower to estimate the direction of the run radiation during each tracking interval. Finally, we also investigate the impact of the shapes and inclination angles of the sensing tower.

4.1 Performance Evaluation on Precision and Energy Harvest

We compare the positions of the sun estimated by Ours, GM, Fixed, and Const against the one calculated by SOLPOS, which we call the *Ideal Case* and is considered as the best case in our simulation. The simulation time is set from 10:00 to 14:00 on May 21, 2011. The sun-tracking procedure is triggered every 15 minutes. GM, which is a bi-axial system, uses four sensing values to estimate the position of the sun. We also use four sensors on our sensing tower for comparison. Hence, the shape of our sensing tower is a regular triangle as shown in Fig. 7. The altitude and azimuth angles of the other sensors are set to (60°, 0°), (60°, 120°), and (60°, 240°), respectively. Besides, we show the original data without curve fitting to GM and our approach. For the Fixed approach, the tilt and azimuth angles of the solar panel are fixed to 28° and 90° (facing to South), respectively. For the Const approach, the tilt angle is also fixed to 28°, and it rotates its solar panel 6° every 15 minutes from East to West with its azimuth angle starting from 30°. The starting tilt and azimuth angles of both GM and our sun-tracking systems are also set to 28° and 30°, respectively.

Each solar panel is assumed to be of size one square meter with an energy generation rate of 8.68 %. The *DST86* stepper motor dst (http://www.tedmotors.com/DST86.htm), which rotates 1.8° per step and requires inputs of 7.6 V, 2.0 A supply, is adopted to rotate solar panels in our simulation. Here, we assume that by DST stepper motors, 10 minutes are required to drive a solar panel to rotate from East to West and 15 minutes to rotate altitude angle from 0° to 90°. We further assume that

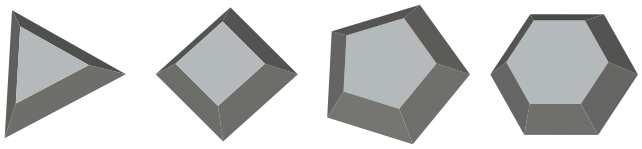

Figure 7: Different shapes of our sensing towers by varying the number of sensors.

a reducer box with 100:1 gear ratio is adopted to allow 0.018° per step, which is sufficient for our objective. Fig. 4 shows our simulation results. In Fig. 4(a), we can see that the performance of our approach on energy generation is very close to the ideal case. Both Fixed and Const approach seem to have good performance, but they cannot predict the overcast conditions. Also, they both suffer worse performance in the afternoon. Fig. 4(b) further shows the total energy gain of these sun-tracking systems. Clearly, the total energy gain of our approach can outperform that of others more than 100000 J/m^2 per day. In addition, our approach can determine the positions of the sun more accurately and quickly. Fig. 4(b) shows that our system has less rotation costs than GM. Fig. 5 shows the estimated altitude and azimuth angles of sun radiation determined by all approaches. The results estimated by our approach are very close to the ideal cases. GM uses bi-axial approach, where four sensors are put on a square shape. The azimuth and altitude angles are estimated by the two sensors deployed on the vertical axis and the horizontal axis, respectively. Hence, GM suffers larger estimated angle errors. The angle deviations can be as large as 57.4° and 57.7°, respectively. Fig. 6 compares the rotation costs. We can see that our approach can provide a stable tracking, and each tracking procedure incurs about 500 rotations and needs about 40 seconds to converge.

4.2 Impact of the Shapes of the Sensing Tower

Here, we discuss the impact of the shapes of the sensing tower on the sun-tracking performance. First, we vary the number of sensors on a sensing tower and measure the total number of tracking procedures invoked by the sensing tower to estimate the position of the sun and the total rotation steps performed by our stepper motors. We vary the number of sensors on the sides of pyramid from 4 to 8 as Fig. 7 shows. The simulation time is also from 9:00 to 16:00 on May 21, 2011, and the precision condition is still set to 0.018°. Also, we set the altitude angles of all side sensors to 60°. In Fig. 8(a), we can see that all shapes have almost the same performance on energy harvesting. This is because our sun-tracking approach can have extremely accurate estimation on sun directions. But as Fig. 8(b) shows, more sensors result in less sun-tracking procedures. Next, we further vary the altitude angles of side sensors from 10° to 70°. Then we discuss the impact on the total number

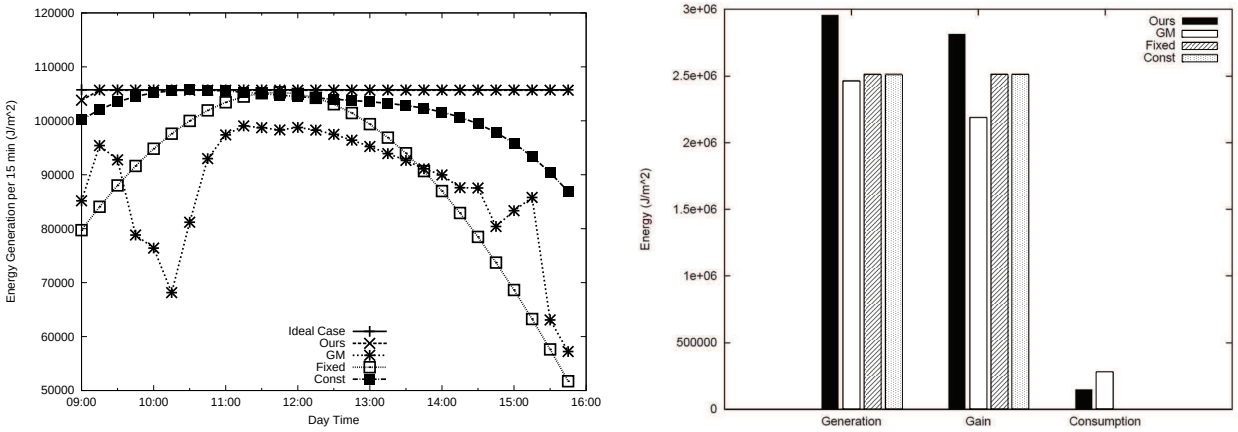

(a) (b)

Figure 4: (a) Comparison on the energy generation per tracking interval. (b) Comparison on the total energy generation, energy consumption, and energy gain.

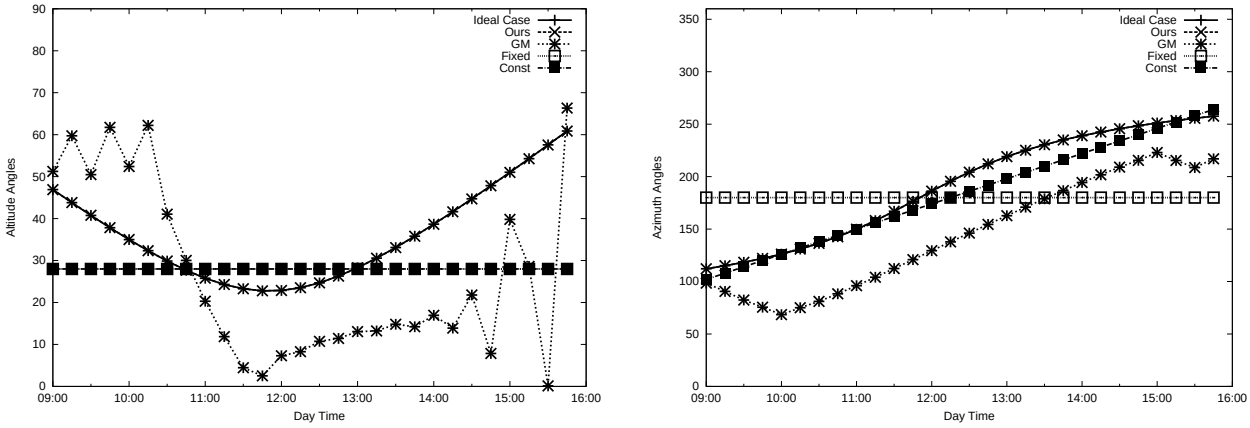

(a) (b)

Figure 5: The estimated positions of the sun: (a) the altitude angles of sun radiation and (b) the azimuth angles of sun radiation.

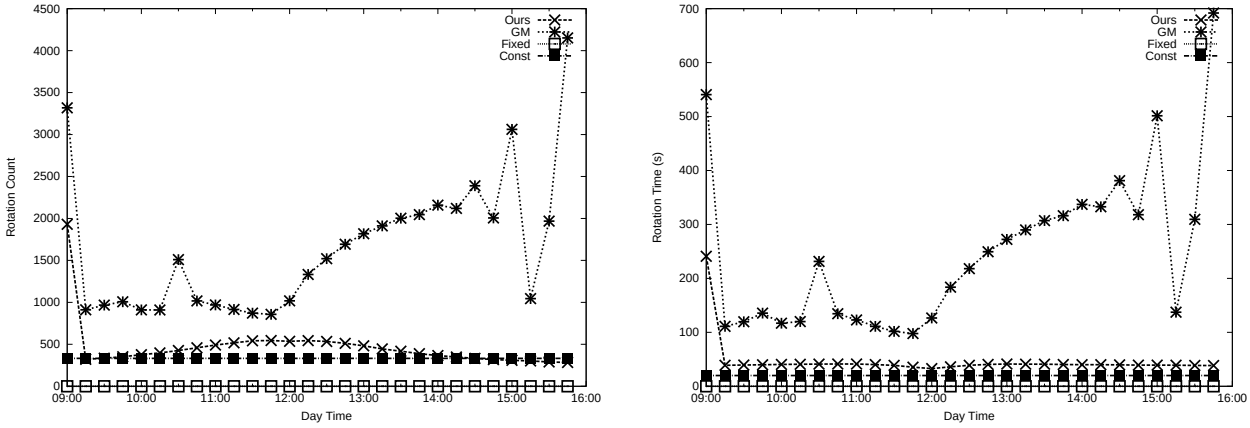

(a) (b)

Figure 6: (a) Comparison on rotation counts. (b) Comparison on rotation cost.

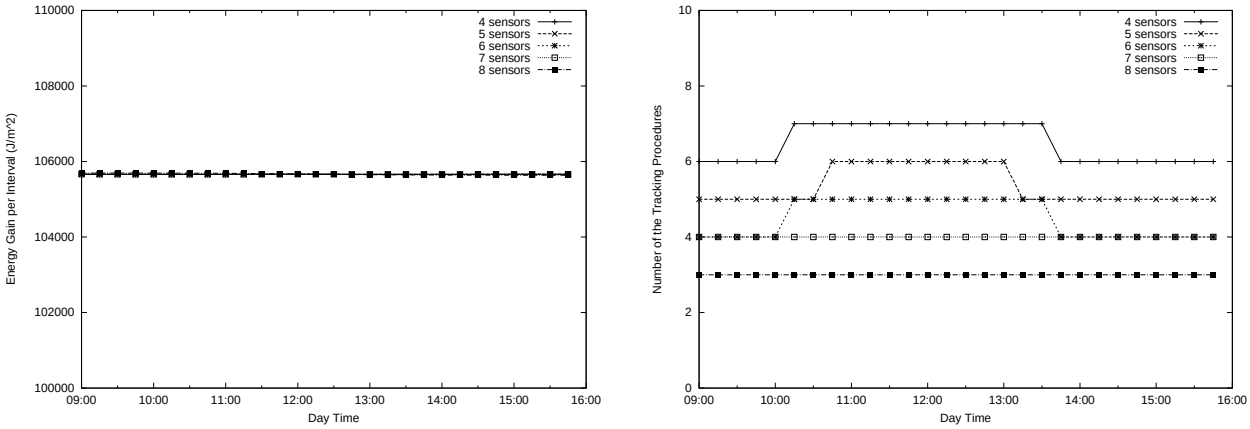

(a) (b)

Figure 8: The impact of the number of sensors on (a) the energy gains and (b) the number of invoked tracking procedures.

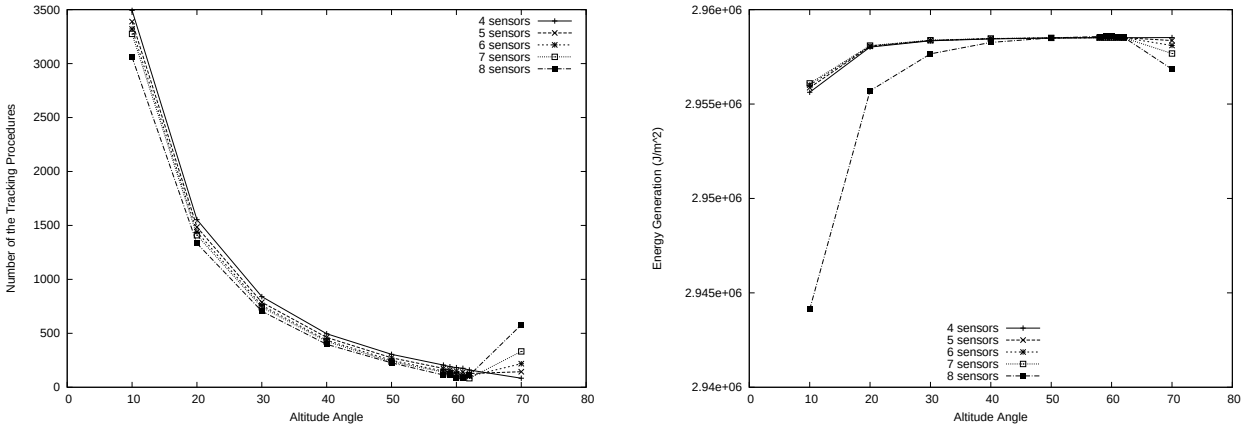

(a) (b)

Figure 9: The impact of the altitude angle of side sensors on (a) the number of invoked tracking procedures and (b) the energy generation.

of tracking procedures invoked by each sensing tower and the total energy generation. Fig. 9 shows that less tracking procedures are needed to tracking the position of the sun when the altitude angle is set close to 60° regardless of the number of sensors in a sensing tower. Also, more sensors result in less tracking procedures. Besides, in Fig. 9(b), we can see that more sensors would produce more energy gains. This is because more sensors can have more accurate estimation on the position of the sun. Furthermore, Fig. 9 shows that our system can have better performance even with only 4 sensors.

5 Prototyping Results

We also build a real prototype to verify our design. There are two main components: the sensing tower and the rotation arm. Fig. 10(a) shows a pyramid-like sensing tower with $k = 5$ sensor. The altitude angle of the 4 side sensors is set to 60°. Each sensor board is built by a microprocessor, a ZigBee module, and a light sensor. Here, we adopt Jennic (JN5139) jennic (http://www.jennic.com/), a single-chip solution for IEEE 802.15.4 802154 (2007) 802154 (2007), and Texas Advanced Optoelectronic Solutions' (TAOS) taos (http://www.taosinc.com/) TSL2650 for light sensing. For the rotation arm part, we use a four-axis robot arm consisting of four Dynamixel AX-12 actuators AX-12 (http://www.crustcrawler.com/motors/AX12/index.php) as our solar panel holder. Each AX-12 actuator can move by 300 degrees in 1024 increments. Therefore, the tracking precision can achieve about 0.3°. Fig. 10(b) and Fig. 10(c) show our robot arm and the Dynamixel AX-12 actuator, respectively. In our design, the coordinator is also implemented with a microprocessor and a wireless module by JN5139 chip, which has a 32-bit RISC processor, a 2.4 GHz IEEE 802.15.4, ZigBee zigbee (http://www.zigbee.org/); Pan et al. (2009) transceiver, 192 KB of ROM, and 96 KB of RAM. Fig. 10(d) shows our coordinator. The sun-tracking algorithm is implemented in the coordinator. As Fig. 10(e) shows, additional PCB board is built up to control the robot arm and it also includes a JN5139 ZigBee module. Hence, after the coordinator determines the rotated angles, it will communicate with the PCB board through the ZigBee protocol. Then the PCB board can control the Dynamixel AX-12 actuators through UART ports. Fig. 10(f) shows the whole tracking system, in which the sensing tower is tied to the solar panel. Therefore, the solar panel and sensing tower will rotate together.

Based on the real implementation, we also conduct some experiments to verify our sun-tracking system. Because the solar irradiation exceeds the limitation of the maximal lux value of TSL2650, whose sensing range is from 0.1 to 40000, we use a LED torch as our light source. Initially, we set the flat top side of our sensing tower parallel to the horizontal plane. Also, we set the altitude angles of the light source to 30°, 45°, and 60°. For comparison, we also use another solar panel with an altitude angle of 30° and an azimuth angle of 0° (North). Then we measure the lux values gathered by the solar panel as our metric. Table 1 shows the results. Because our sun-tracking system can determine the accurate position of the sun, the lux values are almost the same regardless of the direction of light sources. The difference of the lux values are caused by the rotation precision. Small rotation precision of actuators could result in higher tracking precision. Besides, Table 1(a) shows that the lux value decreases as the altitude angle of light sources increases. This is because the distance between the sun-tracking system and the light source is getting larger when the altitude angle becomes larger. Table 1(b) shows the results of the fixed system. Obviously, the maximum lux value only occurs when the altitude angle of the light source is 60° at North.

6 Conclusions

In this paper, we propose a sun-tracking algorithm based on our pyramid-like sensing tower. The proposed sphere-rotated sun-tracking system provides a simple, low-cost, and accurate approach. Also, it gives better decisions for the rotations of solar panels on the overcast weather conditions. By separating the rotation controls of the sensing towers and the solar panels, our model can get better energy gains. Simulation results show that the performance of our system is close to the ideal case on energy gains. Also, our approach outperforms GM and fixed solutions. We further conduct a real prototype with some experiments to verify our approach.

Acknowledgements

Y.-C. Tseng's research is co-sponsored by MoE ATU Plan, by NSC grants 101-2221-E-009-024-MY3, 102-2218-E-009-002, and 102-2923-E-009-001-MY2, by AS-102-TP-A06 of Academia Sinica, by ITRI, Taiwan, and by D-Link.

References

Abdallah (2004) 'The Effect of Using Sun Tracking Systems on The Voltage-Current Characteristics and Power Generation of Flat Plate Photovoltaics.', *Energy Conversion and Management*, Vol. 45, No. 11-12, pp.1671–1679.

Abdallah and Nijmeh (2004) 'Two Axes Sun Tracking System with PLC Control.', *Energy Conversion and Management*, Vol. 45, No. 11-12, pp.1931–11939.

Aiuchi et al. (2006) 'Sensor-Controlled Heliostat with An Equatorial Mount.', *Solar Energy*, Vol. 80, No. 9, pp.1089–1097.

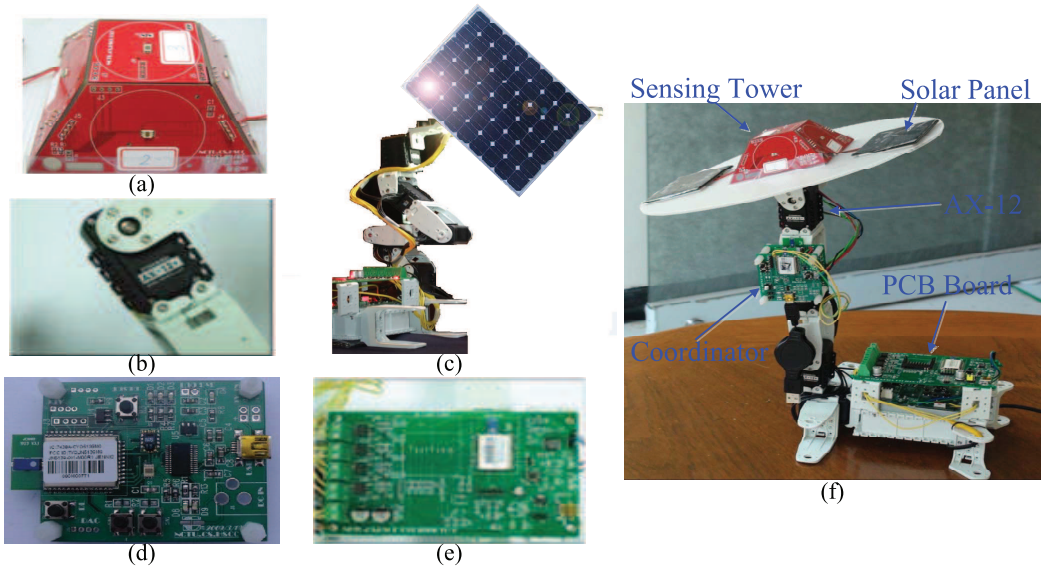

Figure 10: Our sun-tracking prototype, which includes (a) a sensing tower, (b) 4 Dynamixel AX-12 actuators, (c) a robot arm, (d) a coordinator, and (e) a PCB board to control AX-12 actuators. (f) The view of the whole system.

Table 1 Comparison on the lux values obtained by our sun-tracking system against a fixed one.

(a) The lux values obtained by our sun-tracking system.

Azimuth/Altitude angle	N: 0°	E: 90°	S: 180°	W: 270°
30°	2954	2947	2837	2874
45°	2804	2820	2837	2780
60°	2223	2149	2169	2151

(b) The lux values obtained by a fixed system.

Azimuth/Altitude angle	N: 0°	E: 90°	S: 180°	W: 270°
30°	505	406	285	365
45°	2013	1431	410	1324
60°	2165	1135	864	1010

Alippi et al. (2011) 'A robust, adaptive, solar-powered wsn framework for aquatic environmental monitoring.', *IEEE Sensors Journal*, Vol. 11, No. 1, pp.45–55.

Aracil et al. (2006) 'Tracking System for Solar Power Plants.', *IEEE Industrial Electronics Society (IECON)*, pp.3024–3029.

Bakos (2006) 'Design and Construction of A Two-Axis Sun Tracking System for Parabolic trough Collector (PTC) Efficiency Improvement.', *Renewable Energy*, Vol. 31, No. 15, pp.2411–2421.

Berenguel et al. (2004) 'An Artificial Vision-Based Control System for Automatic Heliostat Positioning Offset Correction in A Central Receiver Solar Power Plant.', *Solar Energy*, Vol. 76, No. 5, pp.563–575.

Blanco-Muriel et al. (2006) 'Compute the Solar Vector.', *Solar Energy*, Vol. 70, No. 5, pp.431–441.

Cañada et al. (2007) 'Design of A Sun Tracker for the Automatic Measurement of Spectral Irradiance and Construction of an Irradiance Database in the 330-1100nm Range.', *Renewable Energy*, Vol. 32, No. 12, pp.2053–2068.

Campos et al. (2011) 'Water-displacement-based sun-tracking system to control the orientation of a cylinder parabolic solar concentrator.', *IEEE Electronics, Robotics and Automotive Mechanics Conference (CERMA)*, pp.197–202.

Chenl et al. (2006) 'General sun tracking formula for heliostats with arbitrarily oriented axes.', *Journal of Solar Energy Engineering*, Vol. 128, No. 2, pp.245–250.

Choi et al. (2010) 'Development of A Novel Tracking System for Photovoltaic Efficiency in Low Level Radiation.', *Journal of Power Electronics*, Vol. 10, No. 4, pp.405–411.

Choi et al. (2009) 'General formula for on-axis sun tracking system and its application in improving tracking accuracy of solar collector.', *Solar Energy*, Vol. 83, No. 3, pp.298–305.

Choi et al. (2009) 'Design of A Novel Passive Solar Tracker.', *Solar Energy*, Vol. 77, No. 3, pp.269–280.

Choi et al. (2010) 'Dual axis sun tracking system with pv cell as the sensor, utilizing hybrid electrical characteristics of the cell to determine insolation.', *Proc. of IEEE Int'l Conference on Sustainable Energy Technologies (ICSET)*, pp.1–5.

Choi et al. (2012) 'Use of solar tracking system for extracting solar energy.', *Int'l Journal of Computer and Electrical Engineering*, Vol. 4, No. 1, pp.42–46.

Choi et al. (2010) 'Critical factors that affecting efficiency of solar cells.', *Smart Grid and Renewable Energy*, Vol. 1, No. 1, pp.47–50.

Teco electro devices co., ltd., http://www.tedmotors.com/DST86.htm

AX-12 Dynamixel series robot actuator, http://www.crustcrawler.com/motors/AX12/index.php

Fontani et al. (2011) 'Pointing sensors and sun tracking techniques.', *Int'l Journal of Photoenergy*, pp.1–9.

Grena (2008) 'An algorithm for the computation of the solar position.', *Solar Energy*, Vol. 82, No. 5, pp.462–470.

Han (2011) 'A solar ray automatic tracking device based on image sensor.', *Proc. of Chinese Control Conference (CCC)*, pp.5187–5190.

Huang and Sun (2007) 'Feasibility Study of One Axis Three Positions Tracking Solar PV with Low Concentration Ratio Reflector.', *Energy Conversion and Management*, Vol. 48, No. 4, pp.1273–1280.

IEEE Std 802.15.4 (2006) 'IEEE standard for information technology - telecommunications and information exchange between systems - local and metropolitan area networks specific requirements part 15.4: wireless medium access control (MAC) and physical layer (PHY) specifications for low-rate wireless personal area networks (LR-WPANs)'..

Jennic JN5139, http://www.jennic.com/

Jiao et al. (2010) 'Design of automatic two-axis sun-tracking system.', *Proc. of Int'l Conference on Mechanic Automation and Control Engineering (MACE)*, pp.2323–2326.

Kalogirou (1996) 'Design and Construction of A One-Axis Sun-Tracking System.', *Solar Energy*, Vol. 57, No. 6, pp.465–469.

Kelly and Gibson (2009) 'Improved Photovoltaic Energy Output for Cloudy Conditions with A Solar Tracking System.', *Solar Energy*, Vol. 83, No. 11, pp.2092–2102.

Kelly and Gibson (2009) 'Sun tracking systems: A review.', *Sensors*, Vol. 9, No. 5, pp.3875–3890.

Lorenzo et al. (2002) 'Design of Tracking Photovoltaic Systems with A Single Vertical Axis.', *Progress in Photovoltaics: Research and Applications*, Vol. 10, No. 8, pp.533–543.

Mamlook et al. (2006) 'A Programmable Logic Controller to Control Two Axis Sun Tracking System.', *Information Technology Journal*, Vol. 5, No. 6, pp.1083–1089.

Mamlook et al. (1988) 'The Astronomical Almanac's Algorithm for Approximate Solar Position (1950-2050).', *Solar Energy*, Vol. 40, No. 3, pp.227–235.

Mamlook et al. (2009) 'A Review of Principle and Sun-Tracking Methods for Maximizing Solar Systems Output.', *Renewable and Sustainable Energy Reviews*, Vol. 13, No. 8, pp.1800–1818.

Mwithiga and Kigo (2005) 'Performance of a solar dryer with limited sun tracking capability.', *Journal of Food Engineering*, Vol. 74, No. 2, pp.247–252.

Nuwayhid et al. (2001) 'The Realization of A Simple Solar Tracking Concentrator for University Research Applications.', *Renewable Energy*, Vol. 24, No. 2, pp.207–222.

Oner et al. (2009) 'Design of A New Three-Degree of Freedom Spherical Motor for Photovoltaic-Tracking Systems.', *Renewable Energy*, Vol. 34, No. 12, pp.2751–2756.

Palavras and Bakos (2006) 'Development of A Low-Cost Dish Solar Concentrator and its Application in Zeolite Desorption.', *Renewable Energy*, Vol. 31, No. 15, pp.2422–2431.

Pan et al. (2009) 'The orphan problem in ZigBee wireless networks', *Mobile Computing, IEEE Transactions on*, Vol. 8, No. 11, pp.1583–1584.

Peterson et al. (2005) 'Solar Tracker.', *Technical report, Final Project in Cornell University*, ECE 476.

Ponniran et al. (2011) 'A design of single axis sun tracking system.', *Proc. of Int'l Power Engineering and Optimization Conference (PEOCO)*, pp.107–110.

Photovoltaics PV, http://en.wikipedia.org/wiki/Photovoltaics

Palavras and Bakos (2004) 'Solar Position Algorithm for Solar Radiation Applications.', *Solar Energy*, Vol. 76, No. 5, pp.577–589.

Shibata and Tambo (2010) 'Dual axis light sensor for tracking sun.', *IEEJ Trans. Sensors and Micromachines*, Vol. 130, No. 3, pp.86–91.

Sungur (2009) 'Multi-Axes Sun-Tracking System with PLC Control for Photovoltaic Panels in Turkey.', *Renewable Energy*, Vol. 34, No. 4, pp.1119–1125.

SunPower Corporation, http://us.sunpowercorp.com/

Tang and Bermak (2012) 'An 84 pw/frame per pixel current-mode cmos image sensor with energy harvesting capability.', *IEEE Sensors Journal*, Vol. 12, No. 4, pp.720–726.

Texas Advanced Optoelectronic Solutions, http://www.taosinc.com/

Yang et al. (2009) 'A sun tracking and back-sunlight target detecting system.', *Proc. of Int'l Symposium on Photoelectronic Detection and Imaging : Advances in Imaging Detectors and Applications.*

ZigBee alliance, http://www.zigbee.org/